SUPPLEMENTARY DATA for

Cardiac glycosides are broad-spectrum senolytics

Ana Guerrero, Nicolás Herranz, Bin Sun, Verena Wagner, Suchira Gallage, Romain Guiho, Katharina Wolter, Joaquim Pombo, Elaine E. Irvine, Andrew J. Innes, Jodie Birch, Justyna Glegola, Saba Manshaei, Danijela Heide, Gopuraja Dharmalingam, Jule Harbig, Antoni Olona, Jacques Behmoaras, Daniel Dauch, Anthony G. Uren, Lars Zender, Santiago Vernia, Juan Pedro Martínez-Barbera, Mathias Heikenwalder, Dominic J. Withers and Jesús Gil

Including 7 Supplementary Figures and their corresponding legends

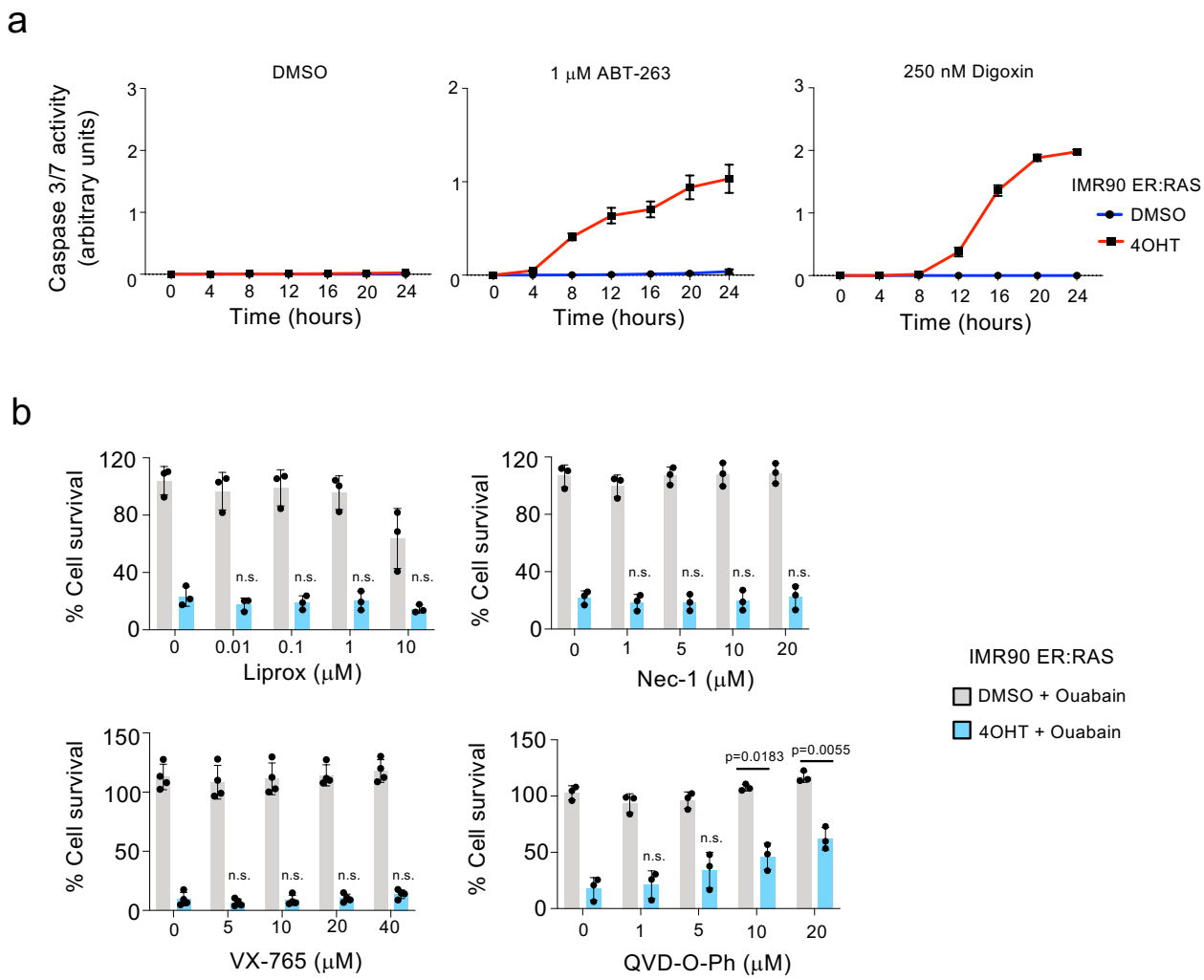

Supplementary Figure 1. Cardiac glycosides induce apoptosis of senescent cells. a, Caspase 3/7 activity in response to vehicle (DMSO), 1 μM ABT-263 or 250 nM digoxin in senescent or control IMR90 ER:RAS cells. IMR90 ER:RAS were treated with 4-OHT or vehicle (DMSO) for 6 days to induce senescence. Senolytics were then added together with NucLight Rapid Red reagent for cell labelling and Caspase-3/7 reagent for apoptosis (IncuCyte). Caspase 3/7 activity was measured at 4 h intervals (*n* = 3). **b**, Quantification of cell survival in senescent and control IMR90 ER:RAS cells after combined treatment of 50 nM ouabain with a ferroptosis inhibitor (liproxstatin-1) (*n* = 3), necroptosis inhibitor (necrostatin-1) (*n* = 3), caspase-1 inhibitor (VX-765) (*n* = 4), or a pan-caspase inhibitor (QVD-O-Ph) (*n* = 3). All error bars represent mean ± s.d; *n* represents independent experiments. All statistical significances were calculated using two-way ANOVA (Dunnett's test); ns, not significant.

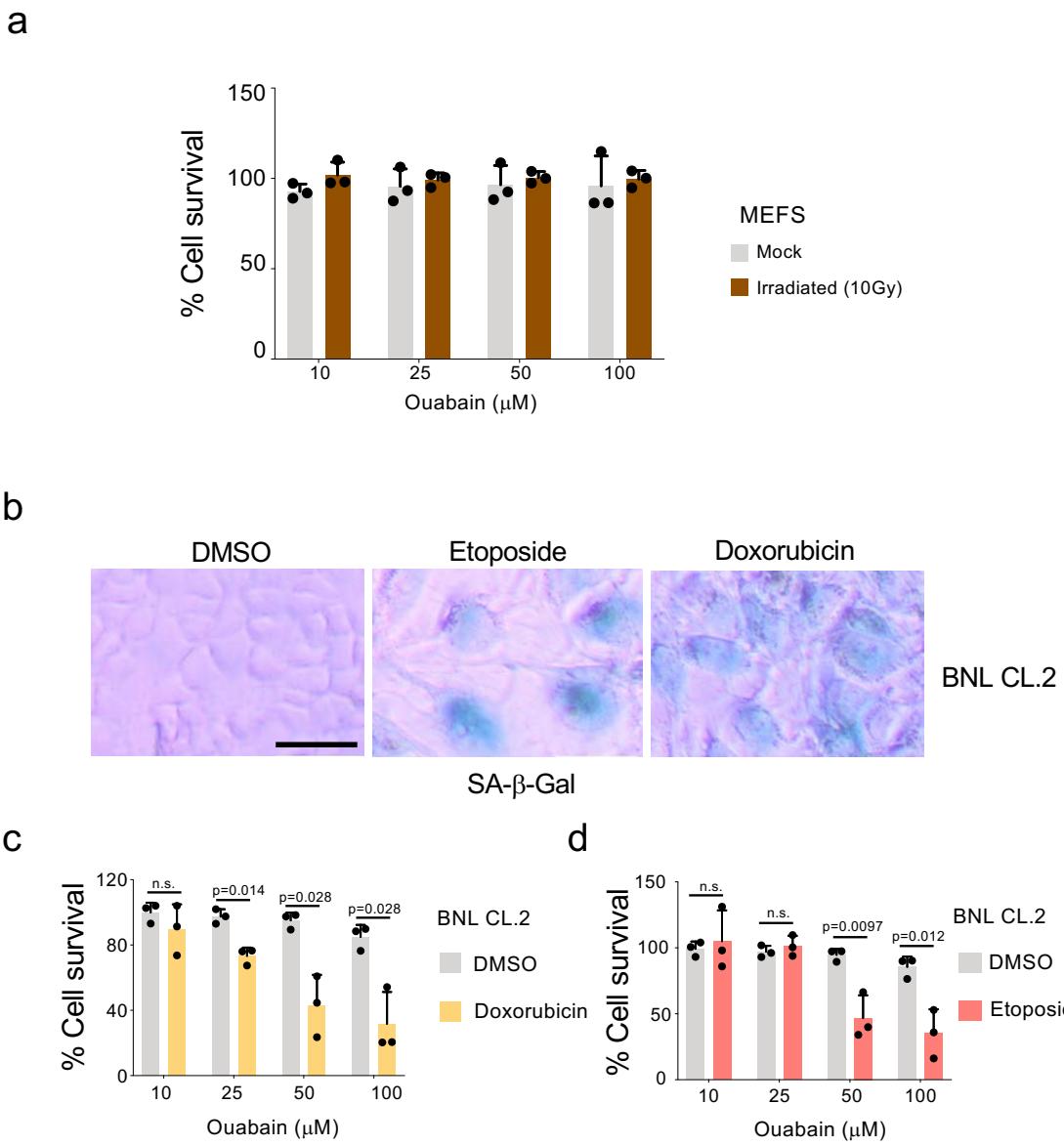

Supplementary Figure 2. Senolytic activity of ouabain in mouse cells. a, Quantification of cell survival of irradiated (10 Gy) or control MEFs after treatment with ouabain (*n* = 3). **b**, Representative images of SA-β-Galactosidase staining of control BNL CL.2 cells and cells treated with etoposide (6.25 μM for 48 hours) or doxorubicin (0.125 μM for 24 hours) on day 8 (*n* = 3). Scale bar 100μm. **c**, Cell survival of senescent *vs* control BNL CL.2 cells after treatment with ouabain at indicated concentrations. Senescence was induced with doxorubicin and ouabain was added from day 6 to day 9 (*n* = 3). **d**, Cell survival of senescent *vs* control BNL CL.2 cells treated with ouabain at indicated concentrations. Senescence was induced with etoposide and ouabain was added from day 6 to day 9 (*n* = 3). All error bars represent mean ± s.d; *n* represents independent experiments. All statistical significances were calculated using unpaired two-tailed Student's *t*-tests; ns, not significant.

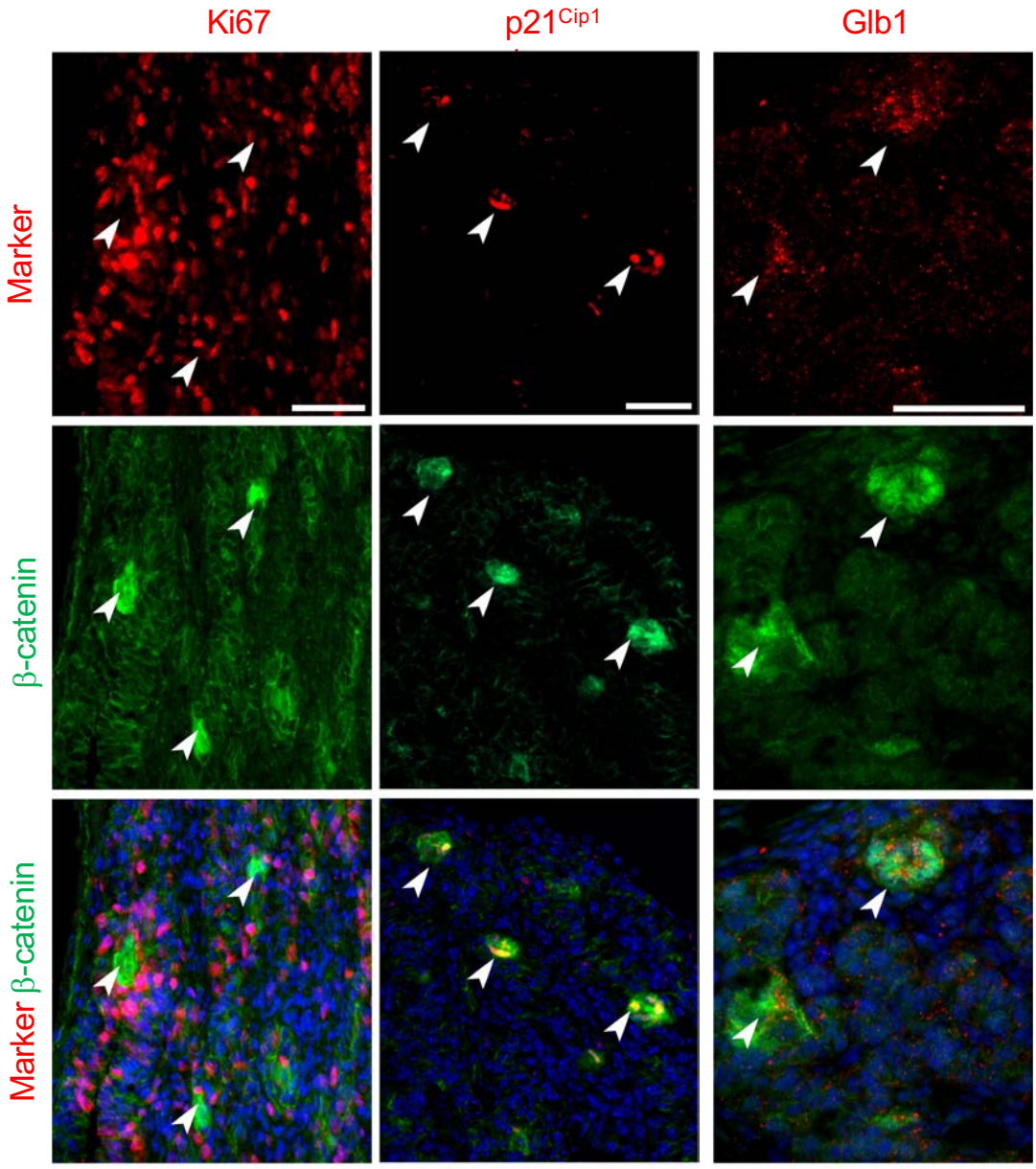

Supplementary Figure 3. β-catenin-positive cells accumulate in clusters and are senescent. Representative images of immunofluorescence staining of β-catenin (green), p21^{Cip1} (red), Ki67 (red) and Glb1 (red) in pituitaries from 18.5dpc *Hesx1$^{Cre/+}$;Ctnnb1$^{lox(ex3)/+}$* mice. Similar results have been described in detail before [37]. Scale bar, 50 μm.

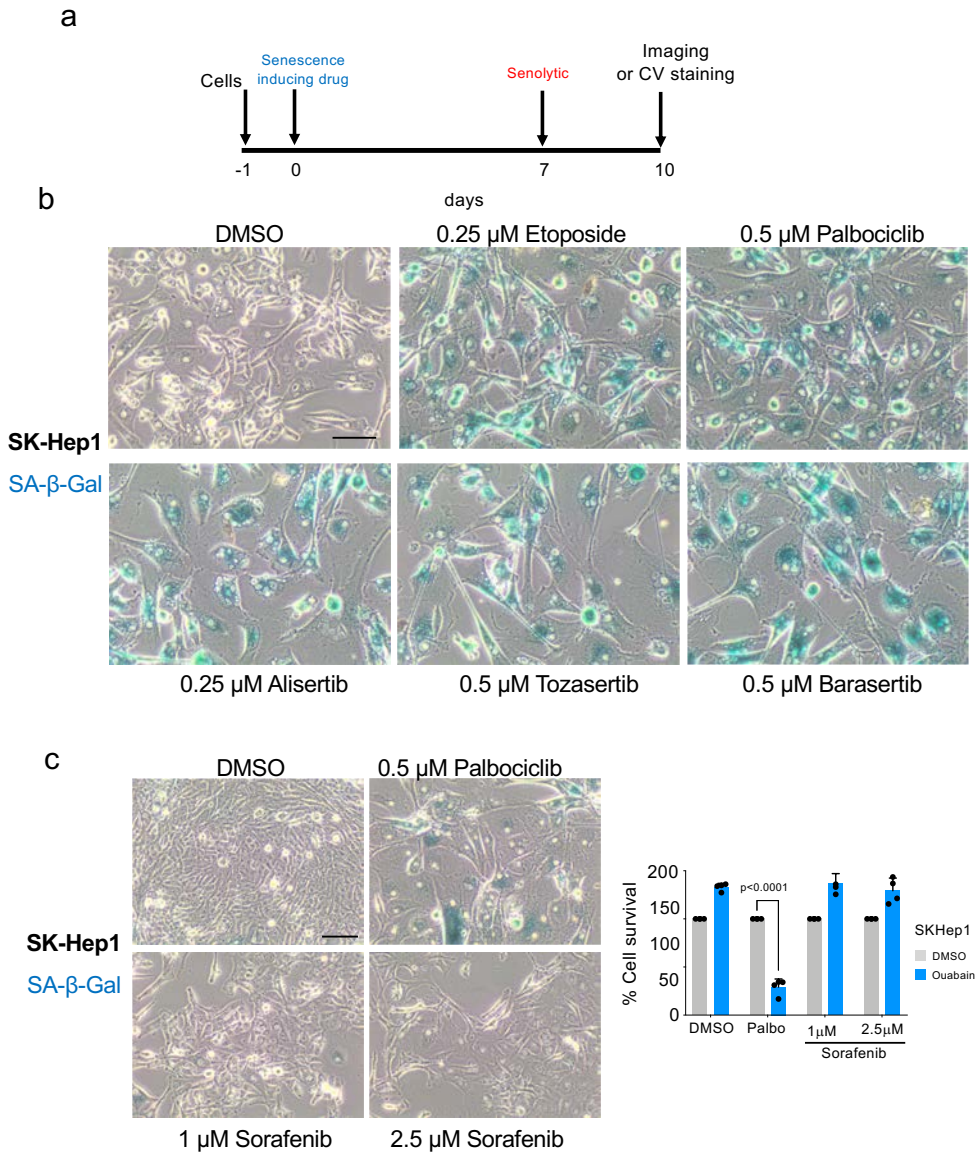

Supplementary Figure 4. Senolytic activity of cardiac glycosides in SK-Hep1 liver cancer cells is dependent on senescence induction. a, Experimental design for the treatment of cancer cells with senescence-inducing anticancer drugs. **b**, Representative pictures of cytochemical SA-β-Gal staining in SK-Hep1 cells undergoing therapy-induced senescence (etoposide, palbociclib, or aurora kinase inhibitors) (*n* = 3). **c**, Representative pictures of cytochemical SA-β-Gal staining in SK-Hep1 cells undergoing therapy-induced senescence (palbociclib) or growth-arrested after treatment with two different concentrations of Sorafenib (left panel). Scale bar, 100 μm. Quantification of cell survival of senescent (palbociclib), growth-arrested (sorafenib) or control (DMSO) SK-Hep1 cells that were subsequently treated with ouabain or vehicle (DMSO) (right panel) (*n* = 4). Statistical significance was calculated using unpaired two-tailed, Student's *t*-test. Data represent mean ± s.d; *n* represents independent experiments.

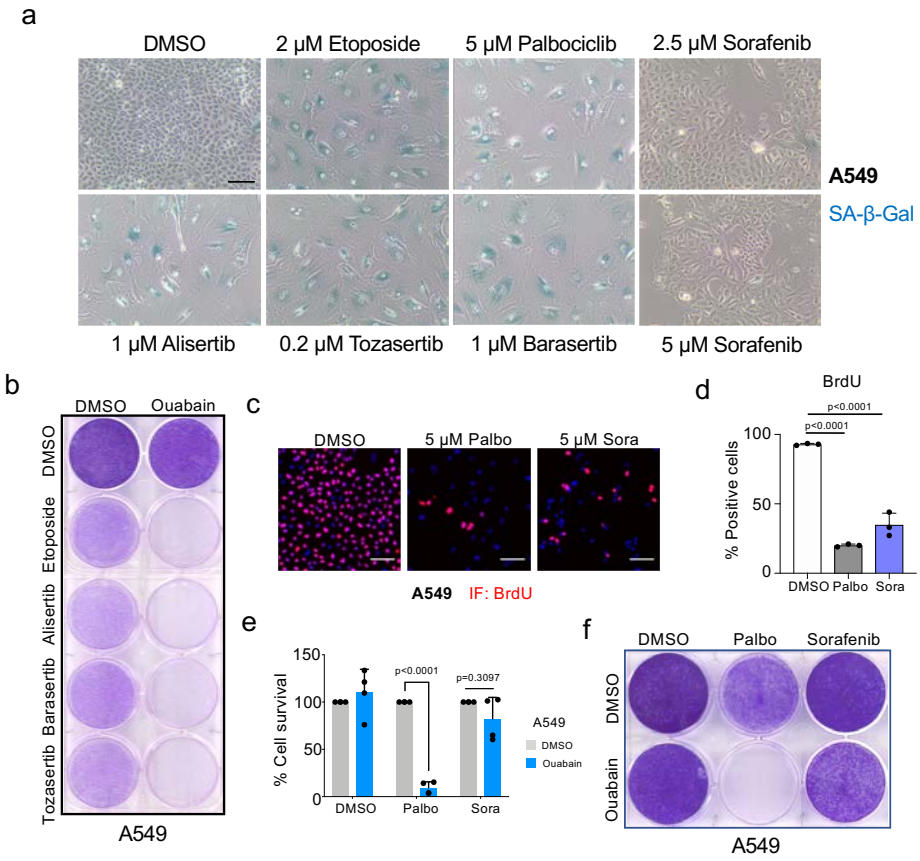

Supplementary Figure 5. Senolytic activity of cardiac glycosides in A-549 lung cancer cells is dependent on senescence induction. a, Representative pictures of cytochemical SA-β-Gal staining in A-549 cells undergoing therapy-induced senescence (etoposide, palbociclib, or aurora kinase inhibitors) or growth-arrested after treatment with two different concentrations of Sorafenib (*n* = 3). Scale bar, 100 µm. **b**, Crystal-violet stained 6-well dishes of A-549 cells that underwent therapy-induced senescence (etoposide, aurora kinase inhibitors) and were subsequently treated with ouabain or vehicle (DMSO) (*n* = 3). **c**, Representative pictures of immunofluorescence (IF) staining for BrdU of A-549 cells 3 days after palbociclib, sorafenib, or vehicle (DMSO). BrdU is stained red. Scale bar, 100 µm. **d**, Quantification of IF staining for BrdU (*n* = 3). Statistical significance was calculated using one-way ANOVA (Dunnett's test). **e**, Quantification of cell survival of senescent (5 µM palbociclib), growth-arrested (5 µM sorafenib) or control (DMSO) A-549 cells that were subsequently treated with ouabain or vehicle (DMSO) (*n* = 3). Statistical significance was calculated using unpaired two-tailed, Student's *t*-test. **f**, Crystal-violet stained 6-well dishes of A-549 cells undergoing therapy-induced senescence (5 µM palbociclib) or growth-arrested (5 µM Sorafenib) that were subsequently treated with ouabain or vehicle (DMSO) (*n* = 3). All error bars represent mean ± s.d; *n* represents independent experiments.

a

b

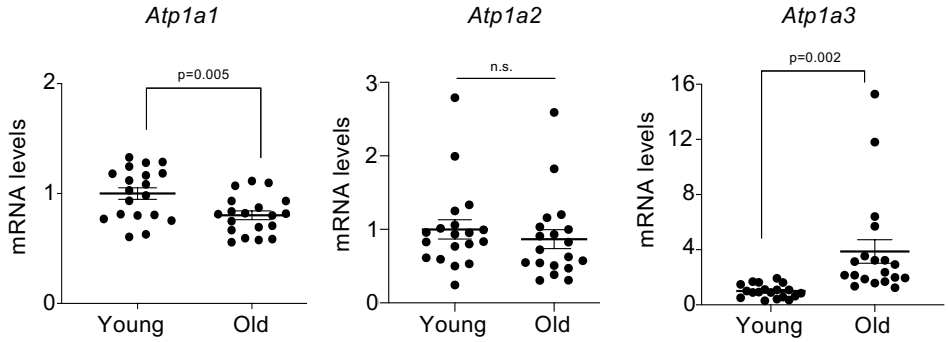

Supplementary Figure 6. Expression of the catalytic subunits of Na^+, K^+ ATPase changes during ageing. **a**, Sequence alignment of indicated sequence of Atp1a1 paralogues. Highlighted are residues 111 and 122 that differ between human and murine (rat, mouse) Atp1a1 and are responsible of increased CG resistance of murine Atp1a1. Mouse Atp1a3 and Atp1a4 have the same residues that human ATP1A1 in positions equivalent to 111 and 122. **b**, Expression levels of *Atp1a1*, *Atp1a2* and *Atp1a3* in liver were determined by qRT-PCR in young (n = 19) and old (n = 19) mice. We could not detect *Atp1a4* by qRT-PCR. Statistical significance was calculated using unpaired two-tailed Student's *t*-test. Data represent mean ± s.e.m.; n represents number of mice; ns, not significant.

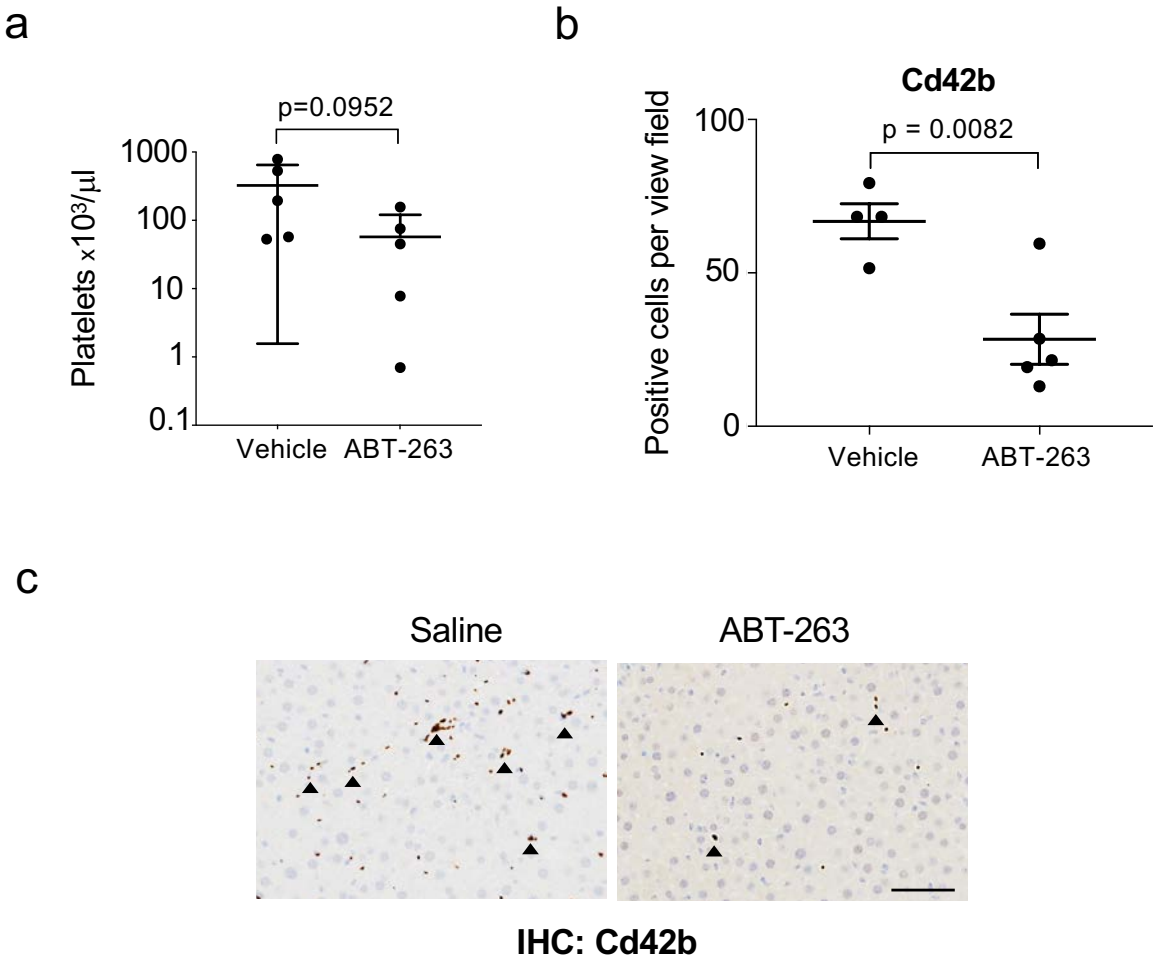

Supplementary Figure 7. Effects of ABT-263 on platelets. Mice were subjected to two rounds of 4 days ABT-263 (50mg/kg by oral gavage daily) with a week break in between. **a**, Platelet count in mice, 6 hours post-treatment of vehicle (*n* = 5) or ABT-263 (*n* = 5). Data represent mean ± s.d. **b**, Quantitative analysis and **c**, representative IHC pictures of Cd42b positive cells in the liver of mice treated with ABT-263 (*n* = 5) or vehicle (*n* = 4). Arrows indicate platelets (Cd42b +). Scale bar, 50 μm. Data represent mean ± s.e.m; *n* represents number of mice. All statistical significances were calculated using unpaired two-tailed Student's *t*-tests.